On the origin of the relative stability of $Zn^{II}NTA$ and $Zn^{II}NTPA$ metal complexes. An insight from the IQA, IQF and π-FARMS methods.

*Paidamwoyo Mangondo and Ignacy Cukrowski**

Department of Chemistry, Faculty of Natural and Agricultural Sciences, University of Pretoria, Lynnwood Road, Hatfield, Pretoria 0002, South Africa

*Corresponding author:

E-mail: ignacy.cukrowski@up.ac.za

Landline: +27 12 420 3988

Supplementary Information

PART S1

Procedure for determining theoretical equilibrium constants for the competition reaction and ball-and-stic representations of relevant lowest energy structures at MP2

The complex formation reactions between zinc and the ligands of interest are shown in equations (S1) and (S2) (charges have been omitted throughout for simplicity)

$$Zn(H_2O)_6 + NTA \leftrightarrow ZnNTA + 4H_2O \qquad K_1^{ZnNTA} = \frac{[ZnNTA]}{[Zn][NTA]} \qquad (S1)$$

$$Zn\ (H_2O)_6 + NTPA \leftrightarrow ZnNTPA + 4H_2O \qquad K_1^{ZnNTPA} = \frac{[ZnNTPA]}{[Zn][NTPA]} \qquad (S2)$$

A competition reaction can be viewed as a combination of the two complexation reactions, (S1) – (S2), in which the ligands NTPA and NTA compete for Zn^{II} and the participation of water is cancelled

$$ZnNTPA + NTA \leftrightarrow ZnNTA + NTPA \qquad K_1^{CRn} = \frac{[ZnNTA][NTPA]}{[ZnNTPA][NTA]} \qquad (S3)$$

Note that K_1^{CRn} can be expressed in terms of K_1^{ZnNTA} and K_1^{ZnNTPA} as

$$K_1^{CRn} = \frac{K_1^{ZnNTA}}{K_1^{ZnNTPA}} = \frac{[ZnNTA][NTPA]}{[ZnNTPA][NTA]} \qquad (S4)$$

hence, the equilibrium constant for the competition reaction, as $\log K_1^{CRn}$, can be determined because the experimental formation constants are known ($\log K_1^{NTA}$ = 10.45 $\log K_1^{NTPA}$ = 5.3) for both complexes,

$$\log K_1^{CRn} = \log \frac{K_1^{NTA}}{K_1^{NTPA}} = \log K_1^{NTA} - \log K_1^{NTPA} = 5.15. \qquad (S5)$$

Considering the well-known relationship which correlates thermodynamic free energy and equilibrium constant, $\Delta G = -RT\ln K$, it is possible to determine the expected from experiment ΔG for the reaction using the conversion factor, 1 log unit = 1.36 kcal mol^{-1}. $\Delta G_{CRn}(aq) = -7.0$ kcal mol^{-1} experimentally. This information is particularly important as one can attempt to approximate this value theoretically by computing the electronic energy of the competition reaction (S3) as

$$\Delta E_{CRn} = E(ZnNTA) + E(NTPA) - E(ZnNTPA) - E(NTA) \qquad (S6)$$

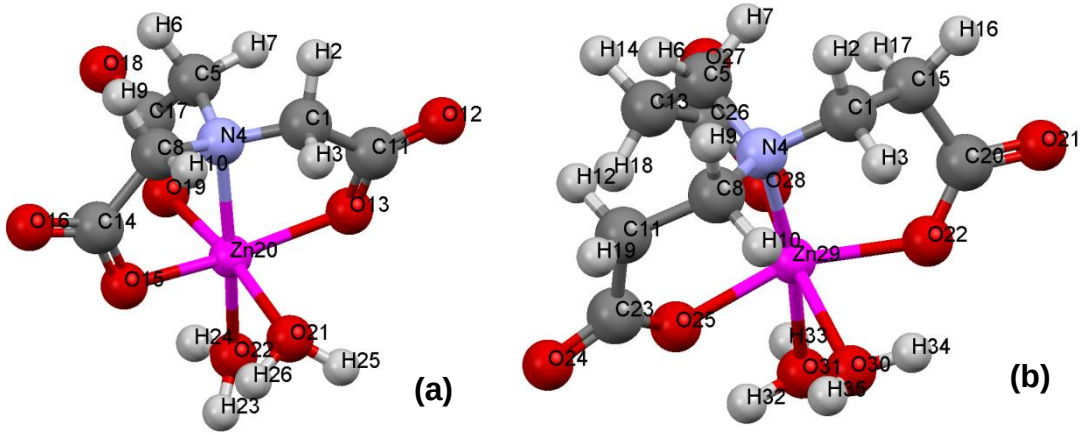

Figure S1. Ball-and-stick representation of the MP2 lowest energy conformers of (a) ZnNTA, and (b) ZnNTPA.

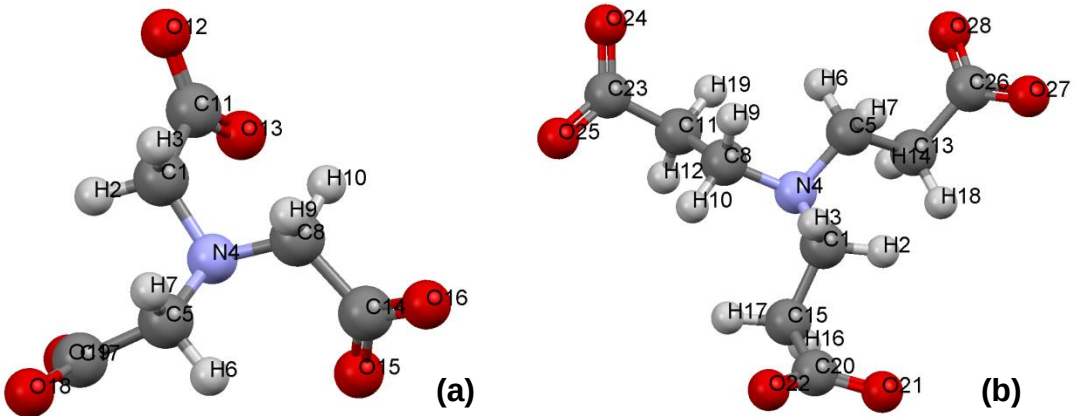

Figure S2. Ball-and-stick representation of the MP2 lowest energy conformers of (a) NTA, and (b) NTPA.

PART S2

Selected topological data in the ZnNTA and ZnNTPA complexes.

Table S1. QTAIM-defined topological data at Critical Points (CPs) of Atomic Interaction Lines (AILs) representing the coordination bonds in ZnNTA and ZnNTPA at the X3LYP[a] level of theory on the MP2 optimized structures.

Bonds	$\rho(r)$	$\nabla^2\rho(r)$	$G(r)$	$V(r)$	$\|V(r)\|/G(r)$	DI(A|B)
			ZnNTA			
Zn–N	0.0688	0.2384	0.0757	–0.0918	1.21	0.31
Zn–O13	0.0676	0.3092	0.0864	–0.0955	1.11	0.33
Zn–O15	0.0677	0.3120	0.0870	–0.0961	1.10	0.33
Zn–O19	0.0679	0.3142	0.0876	–0.0967	1.10	0.33
Zn–O21	0.0446	0.1826	0.0517	–0.0577	1.12	0.21
Zn–O22	0.0537	0.2389	0.0665	–0.0733	1.10	0.26
			ZnNTPA			
Zn–N	0.0692	0.2425	0.0765	–0.0923	1.21	0.34
Zn–O22	0.0724	0.3567	0.0979	–0.1067	1.09	0.35
Zn–O25	0.0699	0.3445	0.0944	–0.1027	1.09	0.34
Zn–O28	0.0699	0.3374	0.0931	–0.1019	1.09	0.34
Zn–O30	0.0327	0.1238	0.0348	–0.0387	1.11	0.15
Zn–O31	0.0441	0.1682	0.0488	–0.0555	1.14	0.21

[a] all values are in au except $|V(r)|/G(r)$ and DI(A|B).

Table S2. QTAIM-defined topological data at ring CPs in ZnNTA and ZnNTPA at the X3LYP[a] level of theory on the MP2-optimized structures.

ZnNTA			ZnNTPA		
Atoms	$\rho(r)$	$\nabla^2\rho(r)$	Atoms	$\rho(r)$	$\nabla^2\rho(r)$
C5-**N4–Zn20–O19**-C17	0.0232	0.1119	C1-**N4–Zn29–O22**-C20-C15	0.0131	0.0578
C1-**N4–Zn20–O13**-C11	0.0215	0.1007	C8-**N4–Zn29–O25**-C23-C11	0.0125	0.0561
C1-**N4–Zn20–O14**-C15	0.0221	0.1041	C5-**N4–Zn29–O28**-C26-C13	0.0125	0.0570
av:	0.0223	0.1056	*av:*	0.0127	0.0570

[a] all values are in au.

Table S3. QTAIM-defined topological data at CPs of AILs representing the weak intramolecular interactions in ZnNTPA at the X3LYP[a] level of theory on the MP2 optimized structures.

Bonds	$\rho(r)$	$\nabla^2\rho(r)$	$G(r)$	$V(r)$	$\|V(r)\|/G(r)$	DI(A|B)
H10•••O30	0.0078	0.0234	0.0053	–0.0047	0.8918	0.0310
H12•••H18	0.0092	0.0331	0.0068	–0.0053	0.7818	0.0126
H18•••O25	0.0096	0.0300	0.0067	–0.0058	0.8761	0.0317
H7•••H17	0.0134	0.0514	0.0105	–0.0081	0.7749	0.0241

[a] all values are in au except $|V(r)|/G(r)$ and DI(A|B)

Origin of Strain in the Coordination Sphere from the NCI perspectives

Combined geometric (d(X,Y)), NCI (isosurfaces) and IQA ($E_{\text{int}}^{\text{X,Y}}$) data are shown in Table S4. Figure S3 shows the NCI-isosurfaces for the ZnNTA and ZnNTPA complexes. Detailed discussion of the IQA data is in the main body of the text, our focus here is primelarly on topological properties.

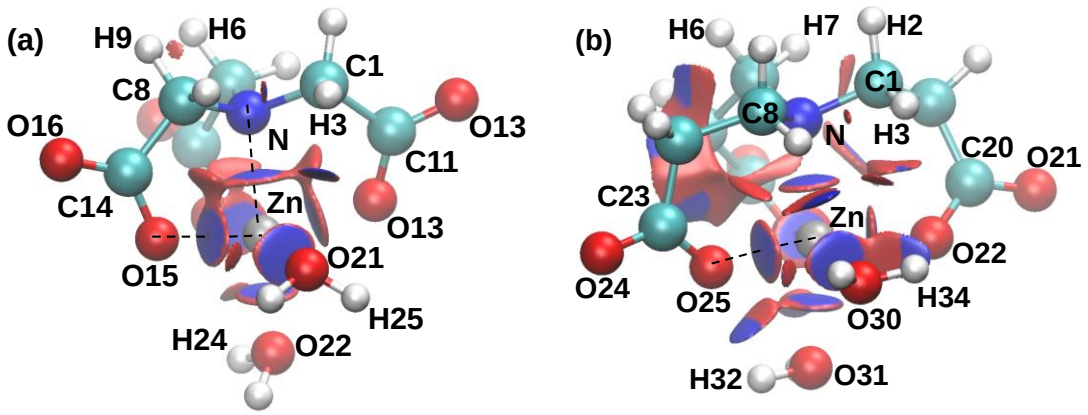

Figure S3. The NCI isosurfaces of the LECs of (a) ZnNTA, and (b) ZnNTPA with a RDG isovalue of 0.5 au and isosurfaces coloured from blue to red using –0.07 au ≤ sign(λ_2)×$\rho(r)$ ≤ +0.03 au.

Table S4. Geometric, NCI and IQA properties of repulsive interactions in the coordination spheres of ZnNTA and ZnNTPA at the X3LYP[a] level of theory on the MP2 optimized structure. Only data for atoms with d(X,Y) < sum of van der Waals radii is included.

Interaction (X•••Y)	d(X,Y)	*NCI*	$E_{\text{int}}^{\text{X,Y}}$	Interaction (X•••Y)	d(X,Y)	*NCI*	$E_{\text{int}}^{\text{X,Y}}$
	ZnNTA				ZnNTPA		
N•••O13(b)	2.709	red-RCP	148.9	N•••O22(b)	3.087	red-RCP	130.4
N•••O15(b)	2.772	red-RCP	147.5	N•••O25(b)	3.016	red-RCP	133.6
N•••O19(b)	2.812	red-RCP	146.1	N•••O28(b)	3.050	red-RCP	133.0
O19(b)•••O15(b)	3.001	None	155.3	O30(w)•••O22(b)	2.667	Red	154.2
O21(w)•••O13(b)	2.886	None	147.3	O30(w)•••O25(b)	2.881	Red	148.8
O21(w)•••O15(b)	2.823	Red	149.5	O31(w)•••O25(b)	2.749	Red	153.7
O22(w)•••O19(b)	2.813	Red	148.4	O31(w)•••O28(b)	2.820	Red	152.1
		Sum:	**1043.0**			**Sum:**	**1005.8**

[a]d(X,Y) is the interatomic distance measured in Å, and $E_{\text{int}}^{\text{X,Y}}$ is the IQA interaction energy between the two atoms, in kcal mol^{-1}.

Note that the O•••O are more repulsive than O•••N interactions and particularly so in ZnNTPA and the N•••O interactions are significantly more repulsive in ZnNTA and this might be attributed to interatomic distances, d(N,O), which are between 0.25-0.35 Å shorter than in

ZnNTPA. Typically, the repulsive O•••O and N•••O interactions are seen as steric contacts. The NCI-defined red isosurface in the interatomic region for, *e.g.*, O25(b)•••O31(w) in ZnNTPA with $V_{XC}^{O,O}$ = –7.6 kcal/mol or N•••O15(b) in ZnNTA with $V_{XC}^{O,O}$ = –5.2 kcal/mol are observed – see Table S5. This is indicative of local electron density depletion and is synonymous with strain within interatomic region. Interestingly, there are two O•••O interactions in ZnNTA, O19(b)•••O15(b) with $V_{XC}^{O,O}$ = –4.5 kcal/mol and O21(w)•••O13(b), with $V_{XC}^{O,O}$ = –5.6 kcal/mol which do not show such density depletion, thus indicating a uniform density distribution in the interatomic region (red isosurfaces are absent) despite a large repulsive interaction energy $E_{int}^{O,O}$ of +151±4 kcalmol^{-1} and very much the same in value exchange-correlation term as found for interactions with red isosurfaces – see Table S4 and S5. Note also that the largest $E_{int}^{O19(b),O15(b)}$ value of +155.3 kcal mol^{-1} is in ZnNTA, even though the interatomic distance *d*(O19(b),O15(b)) of 3.00 Å is the largest among all O•••O interactions. For this interaction $V_{XC}^{O,O}$ = –4.5 kcal mol^{-1} and no NCI isosurface is observed. The data in Table S5 clearly shows that these descriptors (*d*(X,Y), NCI-coloured isosurface, $V_{XC}^{X,Y}$, and $E_{int}^{X,Y}$) do not have to correlate with each other. All the above can be used as an excellent textbook example illustrating the fact that a repulsive interaction, $E_{int}^{X,Y}$ > 0, is not synonymous with intramolecular strain as uncovered by NCI in the form of red isosurfaces, regions with depleted density in a response to a crowded molecular environment to minimize strain.

Just for completeness and clarity, large blue disc-like isosurfaces seen between a central metal ion and donor atoms in Figure S3 represent density accumulations expected from the coordination bond formation. Moreover, formation of the coordination bonds results in the three chelating rings in both complexes. The corresponding red NCI-defined isosurfaces are observed in the region of ring critical points. They are in the form of red (i) cigar-like separate isosurfaces in ZnNTPA and (ii) and discs in ZnNTA; note that due to highly crowded environment, they are attached to blue discs attributed to coordination bond formation.

Classically, complex stability has been associated with the repulsion between lone-pair donor atoms coordinating to the central metal cation. As such, we have fully recovered this notion through highly positive, hence repulsive $E_{int}^{X,Y}$ values (X,Y = O,N). However, from the analysis of the NCI-isosurfaces we noted with interest that the mechanism for responding to a crowded coordination environment is different between the Be^{II} and the Zn^{II} complexes. The interatomic

Table S5. IQA partitioning of two-bodied interaction energies in ZnNTA and ZnNTPA for selected interactions of interest using the XL3YP wavefunction on the MP2 structures.

ZnNTA				ZnNTPA			
Interaction	$V_{cl}^{X,Y}$	$V_{XC}^{X,Y}$	$E_{int}^{X,Y}$	Interaction	$V_{cl}^{X,Y}$	$V_{XC}^{X,Y}$	$E_{int}^{X,Y}$
Coordination bonds between Zn and donor atoms in NTA/NTPA							
Zn–N	–226.9	–46.3	–273.2	Zn–N	–221.1	–50.9	–272.0
Zn–O13$^-$	–251.5	–48.8	–300.2	Zn–O22$^-$	–258.6	–52.5	–311.1
Zn–O15$^-$	–252.2	–48.6	–300.8	Zn–O25$^-$	–256.6	–50.2	–306.8
Zn–O19$^-$	–253.6	–48.3	–301.9	Zn–O28$^-$	–257.0	–50.9	–307.9
Sum-1:	–984.2	–192	–1176.1	Sum-1:	–993.3	–204.5	–1197.8
Coordination bonds with water molecules							
Zn–O21H$_2$	–220.3	–29.9	–250.2	Zn–O30H$_2$	–209.7	–20.0	–229.7
Zn–O22H$_2$	–231.0	–37.4	–268.3	Zn–O31H$_2$	–226.7	–28.7	–255.4
Sum-2:	–451.3	–67.3	–518.5	Sum-2:	–436.4	–48.7	–485.1
Total-1:	–1435.5	–259.1	–1694.7	Sum:	–1429.7	–253.2	–1682.9
Interactions between donor atoms in NTA/NTPA							
N•••O13$^-$	155.2	–6.2	148.9	N•••O22$^-$	133.0	–2.6	130.4
N•••O15$^-$	152.7	–5.2	147.5	N•••O25$^-$	137.0	–3.4	133.6
N•••O19$^-$	150.3	–4.2	146.1	N•••O28$^-$	136.1	–3.1	133.0
O13$^-$•••O15$^-$	116.9	–0.1	116.8	O22$^-$•••O25$^-$	118.8	–0.1	118.7
O13$^-$•••O19$^-$	149.6	–2.6	147.0	O22$^-$•••O28$^-$	158.0	–3.6	154.5
O15$^-$•••O19$^-$	159.8	–4.5	155.3	O25$^-$•••O28$^-$	149.9	–1.9	148.0
Sum-3:	884.5	–22.9	861.6	Sum-3:	832.8	–14.7	818.1
Interactions between donor atoms in NTA/NTPA and O-atoms of water molecules							
N•••O21H$_2$	114.4	–0.9	113.5	N•••O30H$_2$	110.0	–0.7	109.3
N•••O22H$_2$	91.7	–0.1	91.7	N•••O31H$_2$	87.4	0.0	87.4
O13$^-$•••O21H$_2$	152.9	–5.6	147.3	O22$^-$•••O30H$_2$	163.4	–9.2	154.2
O13$^-$•••O22H$_2$	134.7	–2.1	132.6	O22$^-$•••O31H$_2$	140.9	–3.0	137.9
O15$^-$•••O21H$_2$	156.1	–6.7	149.5	O25$^-$•••O30H$_2$	154.7	–5.9	148.8
O15$^-$•••O22H$_2$	137.4	–2.1	135.3	O25$^-$•••O31H$_2$	161.4	–7.6	153.7
O19$^-$•••O21H$_2$	104.0	0.0	104.0	O28$^-$•••O30H$_2$	102.6	0.0	102.6
O19$^-$•••O22H$_2$	154.5	–6.1	148.4	O28$^-$•••O31H$_2$	158.9	–6.8	152.1
Sum-4:	1045.9	–23.5	1022.3	Sum-4:	1079.3	–33.3	1046.0
Interactions between O-atoms of water molecules							
H$_2$O21•••O22H$_2$	138.9	–3.6	135.3	H$_2$O30•••O31H$_2$	134.2	–3.4	130.8
Total-2:	2069.3	–50.0	2019.3	Total-2:	2046.3	–51.4	1994.9
Total-3:	633.7	–309.1	324.6	Total-3:	616.6	–304.6	312.0

[a] Sum-1 stands for summed interaction energies and components of all coordination bonds with NTA/NTPA, Sum-2 stands for summed interaction energies and components of all coordination bonds with O-atoms of the water molecules, Sum-3 stands for summed interaction energies between O$^-$ and N atoms of the coordination spheres, Sum-4 stands for summed interaction energies and components between donor atoms in NTA/NTPA and O-atoms on water molecules, Total-1 stands for summed interaction energies and components of all coordination bonds, Total-2 stands for summed interaction energies and components of all repulsive interactions in the coordination sphere, and Total-3 stands for the summed attractive and repulsive interaction energies and components between all atoms in the coordination sphere.

distances between O(b)-atoms in Be^{II} complexes are significantly shorter than those in Zn^{II} complexes. In response to more crowded atomic environment, some electron density is removed from heteroatoms (their charge decreases) and some is accumulated in the interatomic region (shown as blue isosurfaces); both processes minimize the large electrostatic repulsion between these atoms.[14] The opposite is observed in Zn^{II} complexes where the larger interatomic distances between N- and O(b)-atoms prevent free pairs of electrons overlapping and depletion of electron density is the preferred mechanism. As an example see in Figure S3 the red isosurface between O25(b) and O31(w) in ZnNTPA with a blue adjacent region where the "excess" of density was placed outside coordination sphere and shared with H-atoms of the water molecule, *i.e.*, O25(b)•••H32, resulting in intramolecular H-bonding in ZnNTPA.

Clearly, the main strength of NCI is in identifying regions of non-uniform density distribution, as either accumulation or depletion. However, orthodox interpretations of these regions in terms of atoms being involved in attractive/repulsive interactions can often be misleading and indeed incorrect unless it is supported by IQA-defined interaction energy. To this effect, considering deformation in the density distribution as a measure of intra-coordination strain, it could be concluded that ZnNTA is significantly less strained as two contacts between O-atoms do not have red NCI isosurfaces. However, as shown in Table S5, summed interaction energies produced +1043 kcal mol^{-1}, which is about 37 kcal mol^{-1} larger when compared with ZnNTPA. From data in Table S5 we found that:

- The repulsive interactions within the entire coordination region, which involve N•••O(b), N•••O(w), O(b)•••O(b), O(b)•••O(w), and O(w)•••O(w), do not show a consistent trend; hence, it is impossible to relate these interactions to the preferential complex stability.
- The presence/absence of a short contact, or the presence/absence of an NCI-isosurface, is not indicative of the relative strength of an interaction. Clearly, to describe the nature and strength of an interaction one must analyse the electrostatic, $V_{\mathrm{cl}}^{\mathrm{X,Y}}$, and exchange-correlation, $V_{\mathrm{XC}}^{\mathrm{X,Y}}$, components of the IQA-defined interaction energy between X and Y atoms.

PART S3

A QTAIM and NCI interpretation of the preorganization of the ligand fragments

The previous section focused on the overall energy contributions of fragment preorganization and the binding between the $\mathcal{L}_p$ and $\mathcal{M}_p$. To gain further insight into the sources of strain during preorganization we will use QTAIM, NCI and IQA techniques. We begin by analysing the topological properties in the preorganized ligands. The molecular graphs of the $\mathcal{L}_p$-structures of NTPA and NTA are shown in Figure S4(a-b) and the corresponding NCI isosurfaces are shown in Figure S4(c-d).

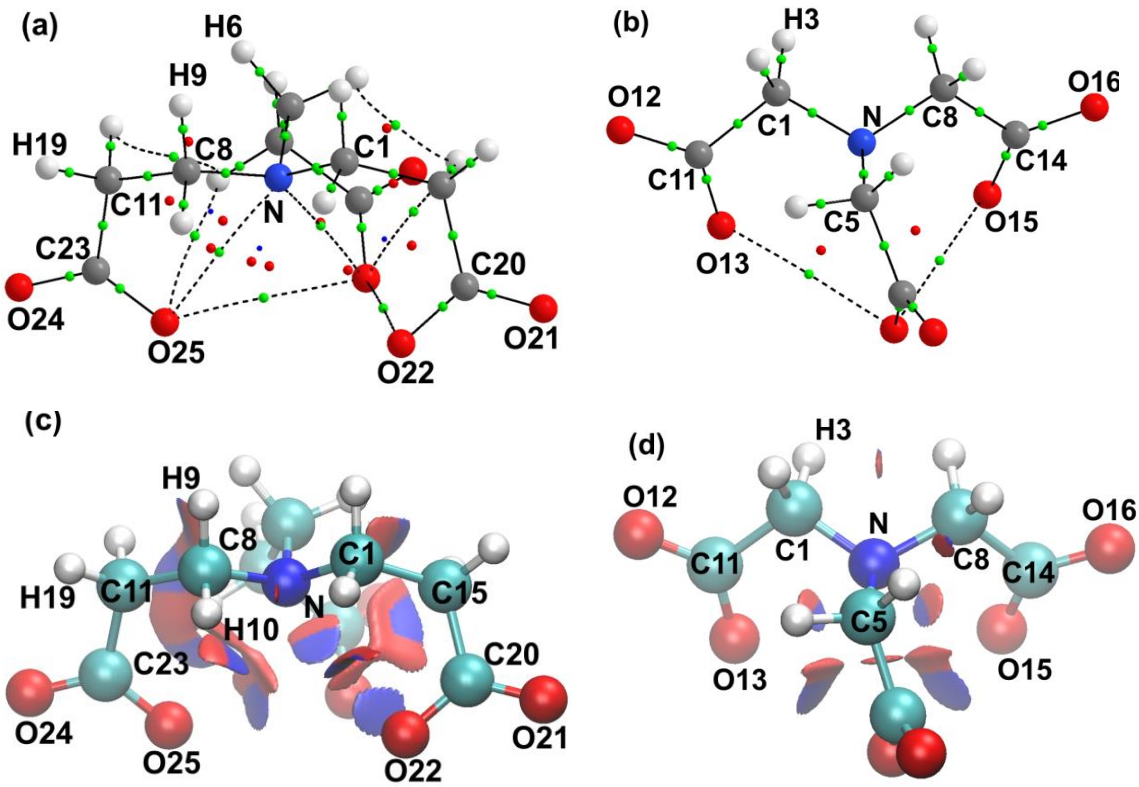

Figure S4. The QTAIM molecular graphs of ligands as found in (a) $\mathcal{L}_p^{NTPA}$, and (b) $\mathcal{L}_p^{NTA}$, as well as the NCI isosurfaces of (c) $\mathcal{L}_p^{NTPA}$, and (d) $\mathcal{L}_p^{NTA}$, with a RDG isovalue of 0.5 au and isosurfaces coloured from blue to red using $-0.07 \leq \text{sign}(\lambda_2)\rho \leq +0.03$

The molecular graphs of the preorganized ligands reveal unexpected atomic interaction lines (AILs) in the highly repulsive coordination sphere, ρ_{CP}(O19--O15) of 0.0091 and ρ_{CP}(O28--O22) of 0.0080 au in NTA and NTPA, respectively. Interestingly, there are no AILs present between the coordinating O-atoms which are furthest apart in both complexes, *e.g.* O22 and O25 in NTPA, where the repulsion is likely to be at a minimum. This is counter intuitive and makes

the classical interpretation of an AIL as a bonding interaction somewhat difficult. It is important to recall that AILs, as clearly explained by Bader, must not be seen or interpreted as chemical bonds. However, it reasonable to postulate that in the region of the most significant repulsion (interatomic distances are shortest), the AIL minimizes the repulsion between the atoms. The AIL becomes a means of dissipating electron density, reducing electrostatic repulsion between the atoms, and simultaneously introducing an exchange correlation term (the presence of an AIL corresponds to the presence of an XC-term), which is always negative. Thus an increase in the XC-term and a decrease in electrostatic repulsion minimizes strain.

The molecular graph of NTPA reveals the presence of additional QTAIM-defined interactions: (i) there are AILs between N--O contacts (ρ_{CP}(N--O25) = 0.0101 and ρ_{CP}(N--O28) 0.0093 au) between the shortest contacts, suggesting that this is a means of minimizing repulsive forces, (ii) there are AILs between H- and O-atoms, indicative of a typical hydrogen bond (ρ_{CP}(H18--O25) 0.0092 and ρ_{CP}(H17--O28) 0.004620 au), and (iii) there are AILs representing CH•••HC interactions (ρ_{CP}(H7--H17) 0.013 and ρ_{CP}(H12--H18) 0.0091 au). Recall that the CH•••O and CH•••HC AILs are also present in the complex (except CH17•••O28). The NCI isosurfaces in Figure S4 correlate with the molecular graphs and all weak intramolecular interactions are fully recovered. There are blue regions of electron density accumulation that correspond to the AILs and red regions of density depletion coinciding with the ring critical and cage critical points. Note there are no isosurfaces between the coordinating O-atoms which are furthest apart. There are additional red isosurfaces between αH-atoms where there were no AILs, and the interatomic distances are incredible small. Traditionally, the NCI interpretation would be to suggest steric hindrance; however, as we have already shown we cannot infer an energetic contribution based on the local density distribution. The density distribution is likely due to the short CH--HC contact and small ring which forces the depletion of density from the local environment. There are additional bi-centric isosurfaces which correspond to the N--O interactions without AILs in both interactions. There are red regions where excess density was removed from the crowded environment and dissipated into the adjacent blue region. Clearly, the interpretation of the molecular graphs and the NCI isosurfaces shown in Figure S4, and particularly in case of NTPA, is not simple and likely speculative as there is no measure of the energetic contributions.

Preorganization of the individual ligand and metal-containing fragments

This section gives a full, in-depth analysis of the preorganization of both the ligand and the metal-containing fragments. Focussing on the groups of chemical significance in the preorganized ligands (N-atoms and atoms in the carboxylate groups) the following pattern emerges: the highly negatively charged atoms, N, γO(b) and γO(nb), experienced a large increase in atomic additive energies whereas the highly positively charged γC-atoms of the carboxylate groups became stabilized the most. The analysis of an intra-atomic contribution $E^{\mathrm{X}}_{\mathrm{self}}$ and interatomic contributions $\sum_{\mathrm{Y}\neq\mathrm{X}} 0.5E^{\mathrm{X,Y}}_{\mathrm{int}}$ and other physical properties shown in Table S6, leads to the following conclusions:

(i) For O(b)- and N-atoms, which will eventually coordinate to the metal atom, the energetic destabilization is due to unfavourable increase in interactions with all remaining atoms in a ligand which is much greater in value than the change in self-atomic energies; $\Delta\sum_{\mathrm{Y}\neq\mathrm{X}} 0.5E^{\mathrm{X,Y}}_{\mathrm{int}}$ >> $|\Delta E^{\mathrm{X}}_{\mathrm{self}}|$. The preorganization of the ligand resulted in the outflow of density, $\Delta N^{\mathrm{X}} < 0$, and the contraction of the atomic volume $\Delta Vol^{\mathrm{X}} < 0$. This was accompanied by a resultant decrease in $\Delta T^{\mathrm{X}} < 0$, reduced electron-electron repulsion, $\Delta V^{\mathrm{XX}}_{\mathrm{ee}} < 0$, and reduced electron-nucleus attraction, $\Delta V^{\mathrm{XX}}_{\mathrm{ne}} > 0$, within the atomic basins. Note that for all N- and carboxylate atoms, if $\Delta N^{\mathrm{X}} < 0$, then $\Delta T^{\mathrm{X}} < 0$, $\Delta V^{\mathrm{XX}}_{\mathrm{ee}} < 0$ and $\Delta V^{\mathrm{XX}}_{\mathrm{ne}} > 0$ and if $\Delta N^{\mathrm{X}} < 0$, then $\Delta T^{\mathrm{X}} > 0$, $\Delta V^{\mathrm{XX}}_{\mathrm{ee}} > 0$ and $\Delta V^{\mathrm{XX}}_{\mathrm{ne}} < 0$. then explain the observed decrease in the self-atomic energy, $\Delta E^{\mathrm{X}}_{\mathrm{self}} < 0$; recall that $E^{\mathrm{X}}_{\mathrm{self}} = T^{\mathrm{X}} + V^{\mathrm{XX}}_{\mathrm{ne}} + V^{\mathrm{XX}}_{\mathrm{ee}}$.

(ii) The converse is noted for the O(nb)-atoms: the change in the additive energy is driven by the destabilization of the self-atomic energies, thus changes in the atomic basins, resulting in $|\Delta\sum_{\mathrm{Y}\neq\mathrm{X}} 0.5E^{\mathrm{X,Y}}_{\mathrm{int}}|$ << $\Delta E^{\mathrm{X}}_{\mathrm{self}}$. The dissipated density from the N- and O- atoms involved in contacts, is accommodated in the accumulation of density in the interatomic region (as shown with NCI isosurfaces and AILs) and the large inflow of density into the

Table S6. Relative from $\mathcal{L}_{\text{free}}$ to $\mathcal{L}_{\text{p}}$, changes in the selected QTAIM- and IQA-(at the RX3LYP level of theory on the MP2 structure) defined energy terms (in kcal mol^{-1}) and additional properties of atoms in ZnNTA and ZnNTPA.[a]

Atom X	$\Delta E^{\text{X}}_{\text{add}}$	$\Delta\sum_{\text{Y}\neq\text{X}} 0.5E^{\text{X,Y}}_{\text{int}}$	$\Delta E^{\text{X}}_{\text{self}}$	ΔT^{X}	$\Delta V^{\text{XX}}_{\text{ne}}$	$\Delta V^{\text{XX}}_{\text{ee}}$	$q^{\text{X}}_{\text{free}}$	$q^{\text{X}}_{\mathcal{L}_{\text{p}}}$	ΔE^{X}	ΔN^{X}	ΔVol^{X}	$\Delta d^{\text{X}}_{\text{e}}$
NTA												
αC8	–0.3	2.1	–2.4	–11.1	27.7	–19.1	0.314	0.319	12.0	–0.005	2.91	–0.0061
αH9	–0.5	–0.4	–0.1	3.1	–3.4	0.2	–0.030	–0.028	–3.1	–0.002	–0.99	0.0003
αH10	0.1	1.7	–1.6	3.8	–9.0	3.6	0.017	–0.002	–3.8	0.019	2.63	–0.0008
γC14	–12.3	–10.7	–1.6	7.6	–20.6	11.5	1.583	1.578	–6.7	0.005	0.82	–0.0023
O15(b)	18.3	35.5	–17.2	–43.2	156.8	–130.8	–1.278	–1.248	45.1	–0.030	–0.83	0.0002
O16(nb)	10.4	–12.2	22.6	49.2	–166.7	140.1	–1.289	–1.321	–47.5	0.032	0.45	0.0000
N4	–0.1	12.7	–12.8	–35.5	158.3	–135.5	–0.959	–0.900	37.0	–0.059	–9.28	0.0128
NTPA												
αC8	–3.8	–0.8	–3.0	–2.7	–7.9	7.6	0.339	0.335	3.8	0.005	0.10	–0.0001
αH9	0.1	–0.3	0.4	7.3	–13.0	6.1	–0.030	–0.053	–7.3	0.023	0.98	0.0000
αH10	0.1	3.1	–3.1	2.8	–8.3	2.4	0.004	–0.017	–2.8	0.021	4.61	–0.0017
βC11	–1.0	0.2	–1.2	–4.6	–3.2	6.7	0.026	0.021	5.7	0.005	–0.45	0.0009
βH12	1.4	–2.2	3.6	0.6	1.5	1.5	–0.010	–0.004	–0.6	–0.006	–4.76	0.0020
βH19	0.1	0.6	–0.5	–2.0	3.5	–2.1	–0.013	–0.012	2.0	–0.001	2.28	–0.0011
γC23	–28.9	–23.6	–5.2	2.3	–19.6	12.0	1.573	1.565	–1.2	0.008	0.57	–0.0015
O24(nb)	17.5	–6.4	24.0	50.3	–183.7	157.4	–1.284	–1.322	–48.2	0.038	–0.37	0.0004
O25(b)	40.1	52.4	–12.2	–35.6	168.7	–145.3	–1.284	–1.236	38.0	–0.048	–7.57	0.0028
N4	19.2	49.4	–30.2	–57.4	346.5	–319.3	–0.969	–0.837	59.2	–0.131	–13.98	0.0173

[a] $E^{\text{X}}_{\text{self}} = T^{\text{X}} + V^{\text{XX}}_{\text{ne}} + V^{\text{XX}}_{\text{ee}}$, by definition; T^{X} - the electronic kinetic energy of an atom (a Hamiltonian form); $V^{\text{XX}}_{\text{ne}}$ - attraction energy between electron density distribution of atom X and nucleus of Atom X; $V^{\text{XX}}_{\text{ee}}$ - two-electron interaction energy of atom X with itself; E^{X} - approximation to a virial-based total energy of atom X; N^{X} - average No of electrons in atom X (atomic electron population); Vol^{X} – atomic volume in bohr^3 (volume bounded by interatomic surfaces of atom X and by isosurface of the electron density distribution (0.001au isodensity surface was used); $d_{\text{e}}^{\text{X}} = N(Vol^{\text{X}})/Vol^{\text{X}}$ - average electron density in Vol^{X} where $N(Vol^{\text{X}})$ is average number of electrons in Vol^{X}.

O(nb) atoms, $\Delta N^{X} > 0$. Consequently, the electron-electron repulsion became more repulsive, $\Delta V_{ee}^{XX} > 0$, and the electron-nucleus attraction became more attractive, $\Delta V_{ne}^{XX} < 0$, in these atoms basins. Although $\left|\Delta V_{ne}^{XX}\right| > \left|\Delta V_{ee}^{XX}\right|$, we see that $\Delta T^{X} > \left|\Delta V_{ne}^{XX} + \Delta V_{ee}^{XX}\right|$ thus the combined effect lead to large increase in the self energies of the O(nb)-atoms.

(iii) Preorganization increased the stability of the highly, positively charged caboxylate C-atoms, $\Delta E_{add}^{X} << 0$. This is largely due to the more attractive molecular environment $\Delta \sum_{Y \neq X} 0.5 E_{int}^{X,Y} << 0$ for NTA and NTPA, stabilizing the interactions with all other atoms. These atoms assist with the dissipation electron density when the ligand goes from $\mathcal{L}_{free}$ to $\mathcal{L}_{p}$ state, by accommodating more electron density, $\Delta N^{X} > 0$, albeit to a lesser extent. The charge re-arrangement in the atomic basin, resulted in similar, in sign (but not magnitude) changes to T^{X}, V_{ne}^{XX} and ΔV_{ee}^{XX}. However, the combined change is such that the self-energies are stabilized, $\Delta E_{self}^{X} < 0$.

There is no immediate or obvious explanation for the preorganization of the metal-containing fragment as there are no additional interactions revealed through QTAIM molecular graphs or NCI isosurfaces. As with the preorganization of the ligand, we decided to trace the origin of preorganization energies from the IQA-perspectives. This reveals that the Zinc atom experiences a large increase in the additive atomic energy, E_{add}^{X}, and thus is highly destabilized. Table S6 shows that additional significant changes occur on two H-atoms. The variation in the additive atomic energies, ΔE_{add}^{X}, (when the metal containing fragment changed from the $(\mathcal{M}_{w})_{f}$ to $(\mathcal{M}_{w})_{p}$ structure) shows that by far more significant changes took place in NTPA. However, regardless of the magnitude of changes, there appears to be a consistent pattern in both systems: Zn, O, and two hydrogen atoms, experienced an increase in atomic additive energies whereas two hydrogen atoms, attached to the equatorial oxygen, became stabilized. The analysis of energy components shown in Table S7 leads to the following conclusions:

(i) The energy destabilization of the positively charged Zn centre, is a result of a destabilizing change in interactions with all other atoms and to a lesser extent the self-atomic energy; $\Delta \sum_{Y \neq X} 0.5 E_{int}^{X,Y} >> \Delta E_{self}^{X}$. Preorganization of the fragment resulted in the dissipation of electron density into the surrounding environment, $\Delta N^{X} < 0$,

Table S7. Relative from $(\mathcal{M}_w)_f$ to $(\mathcal{M}_w)_p$ structures, changes in the selected QTAIM- and IQA-(at the X3LYP level of theory on the MP2 structure) defined energy terms (in kcalmol^{-1}) and additional atomic properties of atoms in ZnNTA and ZnNTPA.

Atom X	ΔE_{add}^{X}	$\Delta\sum_{Y\neq X}0.5E_{int}^{X,Y}$	ΔE_{self}^{X}	ΔT^{X}	ΔV_{ne}^{XX}	ΔV_{ee}^{XX}	q_{free}^{X}	$q_{(\mathcal{M}_w)_p}^{X}$	ΔE^{X}	ΔN^{X}	ΔVol^{X}	Δd_e^{X}
$(\mathcal{M}_w)_p$ (NTA)												
Zn20	10.8	9.6	1.2	–20.4	144.5	–122.9	1.753	1.761	–8.9	–0.008	1.004	–0.0031
O21	0.6	9.7	–9.1	–15.9	54.1	–47.2	–1.152	–1.148	14.7	–0.004	3.788	–0.0020
H25	–5.3	–3.3	–2.0	3.1	–6.1	1.0	0.639	–1.142	–3.2	0.008	0.458	–0.0001
H26	–4.5	–1.8	–2.8	4.2	–8.3	1.3	0.639	0.638	–4.3	0.010	0.669	–0.0001
O22	1.6	5.7	–4.1	–8.2	55.2	–51.1	–1.153	0.631	7.0	–0.011	1.588	–0.0010
H23	3.8	3.8	0.0	0.2	–0.1	–0.1	0.638	0.631	–0.2	0.000	–0.141	0.0001
H24	3.7	5.2	–1.6	2.4	–4.7	0.8	0.637	0.628	–2.4	0.006	0.365	0.0000
$(\mathcal{M}_w)_p$(ZnNTPA)												
Zn29	28.4	20.8	7.6	–44.2	339.5	–287.6	1.753	1.772	–10.7	–0.019	4.785	–0.0141
O30	7.6	22.8	–15.3	–23.8	78.0	–69.5	–1.152	–1.151	21.5	0.000	7.868	–0.0041
H34	–10.0	–4.2	–5.8	8.8	–17.3	2.8	0.639	0.617	–8.8	0.022	1.315	–0.0002
H35	–11.8	–8.6	–3.3	5.2	–10.1	1.6	0.639	0.626	–5.2	0.013	0.847	–0.0002
O31	13.3	25.4	–12.0	–25.5	184.7	–171.3	–1.153	–1.110	23.2	–0.043	1.601	–0.0012
H32	0.6	4.4	–3.8	5.9	–11.5	1.8	0.638	0.623	–5.9	0.015	0.746	0.0000
H33	0.5	3.8	–3.3	5.2	–10.1	1.6	0.637	0.624	–5.2	0.013	0.829	–0.0001

with an expansion of the atomic volume $\Delta Vol^{X} > 0$. The result was less repulsive electron-electron interaction, $\Delta V_{ee}^{XX} < 0$, less attractive electron-nucleus interaction, $\Delta V_{ne}^{XX} > 0$, and less repulsive electronic energy within the atomic basin. The combination of these changes explains the increase in the self-atomic energy, $\Delta E_{self}^{X} > 0$.

(ii) For the O-atoms on the water molecules, observed increase of these atoms additive atomic energies is due to the destabilizing interactions with all other atoms in the fragment and this overrides the decrease in self-energy of these atoms, $\Delta \sum_{Y \neq X} 0.5 E_{int}^{X,Y} > |\Delta E_{self}^{X}|$. During preorganization electron density is dissipated from the negatively charged atoms, $\Delta N^{X} < 0$, and an expansion in the atomic volume was observed $\Delta Vol^{X} > 0$. Because of that, a reduction in the electron-electron repulsion, $\Delta V_{ee}^{XX} < 0$, and the electron-nucleus attraction, $\Delta V_{ne}^{XX} > 0$, within atomic basins is observed. These two changes, in combination with $\Delta T^{X} < 0$, explain the observed decrease in the self-atomic energy, $\Delta E_{self}^{X} < 0$.

Table S8. Relative from $(\mathcal{M}_w)_f$ to $(\mathcal{M}_w)_p$ structures, $\Delta V_{cl}^{X,Y}$, $\Delta V_{XC}^{X,Y}$, and $\Delta E_{int}^{X,Y}$ (at the X3LYP level of theory on the MP2 structure) energy terms (in kcalmol^{-1}) for all diatomic interactions ZnNTA and ZnNTPA.

$(\mathcal{M}_w)_p$ (NTA)					$(\mathcal{M}_w)_p$ (NTPA)				
Atom X	Atom Y	$\Delta V_{cl}^{X,Y}$	$\Delta V_{XC}^{X,Y}$	$\Delta E_{int}^{X,Y}$	Atom X	Atom Y	$\Delta V_{cl}^{X,Y}$	$\Delta V_{XC}^{X,Y}$	$\Delta E_{int}^{X,Y}$
Zn20	O21	11.3	8.5	19.9	Zn29	O30	22.8	17.6	40.4
O21	H23	7.4	0.3	7.7	Zn29	O31	13.1	5.6	18.7
Zn20	H24	5.7	0.1	5.7	O30	H32	13.5	0.4	13.9
Zn20	O22	3.2	1.2	4.4	O31	H35	8.3	0.0	8.3
O21	H25	5.3	–1.9	3.4	O31	H32	12.1	–3.9	8.3
O21	H26	5.8	–2.6	3.2	O31	H33	11.0	–3.2	7.9
O22	H23	2.6	–0.3	2.3	O31	H34	6.9	0.0	6.9
O21	H24	2.0	0.0	2.1	O30	H35	9.3	–3.1	6.2
O22	H24	3.0	–1.5	1.4	O30	H34	10.8	–5.5	5.3
H23	H26	1.1	0.0	1.1	O30	H33	3.6	0.0	3.7
H24	H25	0.9	0.0	0.9	Zn29	H33	3.4	0.1	3.5
H24	H26	0.7	0.0	0.7	Zn29	H32	3.0	0.1	3.1
H23	H25	0.5	0.0	0.5	H33	H34	–1.6	0.0	–1.6
H23	H24	–0.3	0.0	–0.3	H32	H33	–2.6	0.0	–2.6
O22	H26	–2.1	0.0	–2.1	H33	H35	–3.2	0.0	–3.2
H25	H26	–2.2	0.0	–2.3	H34	H35	–4.4	–0.1	–4.5
O22	H25	–2.6	0.0	–2.5	H32	H35	–6.3	0.0	–6.3
Zn20	H23	–3.8	0.0	–3.8	Zn29	H34	–7.1	0.2	–6.9
Zn20	H26	–4.3	0.1	–4.2	H32	H34	–7.6	0.0	–7.6
O21	O22	–6.0	1.6	–4.4	O30	O31	–12.9	1.5	–11.5
Zn20	H25	–6.7	0.0	–6.7	Zn29	H35	–17.6	0.0	–17.6

PART S4

Derivation of the IQA/IQF-based protocol for binding energy decomposition

Let us first express the components of the binding energy, as shown in Eq. (S7), in terms of additive atomic energies,

$$E_{\text{bind}}^{\text{ML}} = \sum_{\text{X}\in\text{ML}} E_{\text{add}}^{\text{X}} - \sum_{\text{X}\in\mathcal{L}_{\text{p}}} E_{\text{add}}^{\text{X}} - \sum_{\text{X}\in(\mathcal{M}_{\text{w}})_{\text{p}}} E_{\text{add}}^{\text{X}} \tag{S7}$$

Recall that the additive energy of an atom is the sum of the self-atomic contribution and the interatomic contributions, thus by substituting $E_{\text{add}}^{\text{X}} = E_{\text{self}}^{\text{X}} + \sum_{\text{Y}\neq\text{X}} 0.5 E_{\text{int}}^{\text{X,Y}}$ into Eq. (S7) the binding energy is

$$E_{\text{bind}}^{\text{ML}} = \sum_{\text{X}\in\text{ML}} E_{\text{self}}^{\text{X}} + 0.5 \sum_{\text{X}\in\text{ML}} \sum_{\substack{\text{X}\neq\text{Y}\\ \text{Y}\in\text{ML}}} E_{\text{int}}^{\text{X,Y}} - \sum_{\text{X}\in\mathcal{L}_{\text{p}}} E_{\text{self}}^{\text{X}} - 0.5 \sum_{\text{X}\in\mathcal{L}_{\text{p}}} \sum_{\substack{\text{Y}\neq\text{X}\\ \text{Y}\in\mathcal{L}_{\text{p}}}} E_{\text{int}}^{\text{X,Y}} - \sum_{\text{X}\in(\mathcal{M}_{\text{w}})_{\text{p}}} E_{\text{self}}^{\text{X}} - 0.5 \sum_{\text{X}\in\mathcal{M}_{\text{p}}} \sum_{\substack{\text{Y}\neq\text{X}\\ \text{Y}\in(\mathcal{M}_{\text{w}})_{\text{p}}}} E_{\text{int}}^{\text{X,Y}} \tag{S8}$$

The first two terms represent the energy of the complex in the primary IQA energy components; the third term represents the self-energies of all atoms in the preorganized ligand which can be written as $E_{\text{self}}^{\mathcal{L}_{\text{p}}}$, self-atomic energy contribution to the energy of the fragment $\mathcal{L}_{\text{p}}$; the fourth term sums up all unique diatomic interaction energies between atoms within the fragment, $\mathcal{L}_{\text{p}}$, and is the intra-fragment interaction energy, $E_{\text{int}}^{\mathcal{L}_{\text{p}}}$. Similarly, $E_{\text{self}}^{(\mathcal{M}_{\text{w}})_{\text{p}}}$ represents the contribution of the self-atomic energies and $E_{\text{int}}^{(\mathcal{M}_{\text{w}})_{\text{p}}}$ represents the intra-fragment energy contribution to the energy of the fragment $(\mathcal{M}_{\text{w}})_{\text{p}}$. The binding energy in Eq. (S8) can be written in fragment notation as

$$E_{\text{bind}}^{\text{ML}} = \sum_{\text{X}\in\text{ML}} E_{\text{self}}^{\text{X}} + 0.5 \sum_{\text{X}\in\text{ML}} \sum_{\substack{\text{Y}\neq\text{X}\\ \text{Y}\in\text{ML}}} E_{\text{int}}^{\text{X,Y}} - E_{\text{self}}^{\mathcal{L}_{\text{p}}} - E_{\text{int}}^{\mathcal{L}_{\text{p}}} - E_{\text{self}}^{(\mathcal{M}_{\text{w}})_{\text{p}}} - E_{\text{int}}^{(\mathcal{M}_{\text{w}})_{\text{p}}}. \tag{S9}$$

During the final formation, all diatomic interactions existing in the framework of the pre-organized fragments ($\mathcal{L}_{\text{p}}$ and $(\mathcal{M}_{\text{w}})_{\text{p}}$) must change to those present in the complex, $\mathcal{L}_{\text{c}}$ which interacts with $(\mathcal{M}_{\text{w}})_{\text{c}}$. As a matter of fact, because of a large density redistribution taking place on complex formation, not only the diatomic interaction energies, but also the self-atomic and additive atomic energies in the each fragment must have changed too. To

understand all the changes taking place in the ligand, it was necessary to further decompose the interaction energy term applicable to the ML complex (second term in Eq. (S9)) into separate contributions coming from (i) interactions between atoms within a ligand framework when in complex, (ii) interactions between atoms with in the metal-containing fragment when in complex, and (iii) all new diatomic interactions in the complex between all atoms in $\mathcal{M}_{\mathrm{w}}$ and all atoms of $\mathcal{L}$, the first, second and third term in Eq. (S10), respectively

$$0.5\sum_{\mathrm{X}\in\mathrm{ML}}\sum_{\substack{\mathrm{X}\neq\mathrm{Y}\\ \mathrm{Y}\in\mathrm{ML}}}E_{\mathrm{int}}^{\mathrm{X,Y}} = 0.5\sum_{\mathrm{X}\in\mathcal{L}_{\mathrm{c}}}\sum_{\substack{\mathrm{Y}\neq\mathrm{X}\\ \mathrm{Y}\in\mathcal{L}_{\mathrm{c}}}}E_{\mathrm{int}}^{\mathrm{X,Y}} + 0.5\sum_{\mathrm{X}\in(\mathcal{M}_{\mathrm{w}})_{\mathrm{c}}}\sum_{\substack{\mathrm{Y}\neq\mathrm{X}\\ \mathrm{Y}\in(\mathcal{M}_{\mathrm{w}})_{\mathrm{c}}}}E_{\mathrm{int}}^{\mathrm{X,Y}} + \sum_{\mathrm{X}\in(\mathcal{M}_{\mathrm{w}})_{\mathrm{c}}}\sum_{\mathrm{Y}\in\mathcal{L}_{\mathrm{c}}}E_{\mathrm{int}}^{\mathrm{X,Y}} \tag{S10}$$

The last term is effectively the interaction energy between two fragments (inter-fragment interaction energy) and in fragment notation we obtain

$$0.5\sum_{\mathrm{X}\in\mathrm{ML}}\sum_{\substack{\mathrm{X}\neq\mathrm{Y}\\ \mathrm{Y}\in\mathrm{ML}}}E_{\mathrm{int}}^{\mathrm{X,Y}} = E_{\mathrm{int}}^{\mathcal{L}_{\mathrm{c}}} + E_{\mathrm{int}}^{(\mathcal{M}_{\mathrm{w}})_{\mathrm{c}}} + E_{\mathrm{int}}^{(\mathcal{M}_{\mathrm{w}})_{\mathrm{c}},\mathcal{L}_{\mathrm{c}}} \tag{S11}$$

Traditionally the focus has been on the coordination bonds, but an inter-fragment interaction energy term analyses all possible interactions between the two fragments. The expansion of the interatomic contributions to the energy of the complex also enables one to define a term that estimates the energy gain/lost as a result of the changes in the intra-fragment interaction energy,

$$\Delta E_{\mathrm{int}}^{\mathcal{L}} = 0.5\sum_{\mathrm{X}\in\mathcal{L}_{\mathrm{c}}}\sum_{\substack{\mathrm{Y}\neq\mathrm{X}\\ \mathrm{Y}\in\mathcal{L}_{\mathrm{c}}}}E_{\mathrm{int}}^{\mathrm{X,Y}} - 0.5\sum_{\mathrm{X}\in\mathcal{L}_{\mathrm{p}}}\sum_{\substack{\mathrm{Y}\neq\mathrm{X}\\ \mathrm{Y}\in\mathcal{L}_{\mathrm{p}}}}E_{\mathrm{int}}^{\mathrm{X,Y}} \tag{S12}$$

and

$$\Delta E_{\mathrm{int}}^{\mathcal{M}_{\mathrm{w}}} = 0.5\sum_{\mathrm{X}\in(\mathcal{M}_{\mathrm{w}})_{\mathrm{c}}}\sum_{\substack{\mathrm{Y}\neq\mathrm{X}\\ \mathrm{Y}\in(\mathcal{M}_{\mathrm{w}})_{\mathrm{c}}}}E_{\mathrm{int}}^{\mathrm{X,Y}} - 0.5\sum_{\mathrm{X}\in(\mathcal{M}_{\mathrm{w}})_{\mathrm{p}}}\sum_{\substack{\mathrm{Y}\neq\mathrm{X}\\ \mathrm{Y}\in(\mathcal{M}_{\mathrm{w}})_{\mathrm{p}}}}E_{\mathrm{int}}^{\mathrm{X,Y}} \tag{S13}$$

These terms estimate the energy pertaining to the rearrangement of intra-fragment interactions within the fragment framework when it moves from the preorganized state ($\mathcal{L}_{\mathrm{p}}$ and $(\mathcal{M}_{\mathrm{w}})_{\mathrm{p}}$) to the final complexed state ($\mathcal{L}_{\mathrm{c}}$ and $(\mathcal{M}_{\mathrm{w}})_{\mathrm{c}}$). In the fragment notation we can express Eq. (S12) as

$$\Delta E_{\mathrm{int}}^{\mathcal{L}} = E_{\mathrm{int}}^{\mathcal{L}_{\mathrm{c}}} - E_{\mathrm{int}}^{\mathcal{L}_{\mathrm{p}}} \tag{S14}$$

And Eq. (S13) as

$$\Delta E_{\text{int}}^{\mathcal{M}_{\text{w}}} = E_{\text{int}}^{(\mathcal{M}_{\text{w}})_{\text{c}}} - E_{\text{int}}^{(\mathcal{M}_{\text{w}})_{\text{p}}} \tag{S15}$$

By making use of expression (S11), (S14) and (S15) and combining contributions coming from self-atomic energies one can express Eq. (S9) in terms of primary energy terms used in the IQA partitioning scheme, self-atomic and diatomic interaction energies, as

$$E_{\text{bind}} = \sum_{\text{X}\in\text{ML}} \Delta E_{\text{self}}^{\text{X}} + \Delta E_{\text{int}}^{\mathcal{I}} + \Delta E_{\text{int}}^{\mathcal{M}_{\text{w}}} + E_{\text{int}}^{(\mathcal{M}_{\text{w}})_{\text{c}},\mathcal{I}_{\text{c}}} \tag{S16}$$

where

$$\sum_{\text{X}\in\text{ML}} \Delta E_{\text{self}}^{\text{X}} = \sum_{\text{X}\in\text{ML}} E_{\text{self}}^{\text{X}} - \sum_{\text{X}\in\mathcal{I}_{\text{p}}} E_{\text{self}}^{\text{X}} - \sum_{\text{X}\in(\mathcal{M}_{\text{w}})_{\text{p}}} E_{\text{self}}^{\text{X}} \tag{S17}$$

which for brevity can be written as

$$\Delta E_{\text{self}}^{\text{ML}} = E_{\text{self}}^{\text{ML}} - E_{\text{self}}^{\mathcal{I}_{\text{p}}} - E_{\text{self}}^{(\mathcal{M}_{\text{w}})_{\text{p}}} \tag{S18}$$

The term $\sum_{\text{X}\in\text{ML}} \Delta E_{\text{self}}^{\text{X}} = \Delta E_{\text{self}}^{\text{ML}}$ defined in Eq. (S17) accounts for the total energy contribution coming from the self-atomic energies of all atoms of the molecular system when the pre-organized ligand and metal fragment bind to form a final complex ML.

To learn about the nature of changes observed in diatomic interactions within each fragment, one can make use of a classical (electrostatic) contribution, $V_{\text{cl}}^{\text{X,Y}}$, and exchange-correlation, XC energy term, $V_{\text{XC}}^{\text{X,Y}}$ which are obtained from the decomposition of a diatomic energy term, $E_{\text{int}}^{\text{X,Y}} = V_{\text{cl}}^{\text{X,Y}} + V_{\text{XC}}^{\text{X,Y}}$. Thus we can isolate the interaction energy rearrangements in the fragment as being of the classical electrostatic and exchange-correlation origin,

$$\Delta E_{\text{int}}^{\mathcal{I}} = \Delta V_{\text{cl}}^{\mathcal{I}} + \Delta V_{\text{XC}}^{\mathcal{I}} \tag{S19}$$

where

$$\Delta V_{\text{cl}}^{\mathcal{I}} = 0.5 \sum_{\text{X}\in\mathcal{I}_{\text{c}}} \sum_{\substack{\text{Y}\neq\text{X} \\ \text{Y}\in\mathcal{I}_{\text{c}}}} V_{\text{cl}}^{\text{X,Y}} - 0.5 \sum_{\text{X}\in\mathcal{I}_{\text{p}}} \sum_{\substack{\text{Y}\neq\text{X} \\ \text{Y}\in\mathcal{I}_{\text{p}}}} V_{\text{cl}}^{\text{X,Y}} \tag{S20}$$

and

$$\Delta V_{\mathrm{XC}}^{\mathcal{L}} = 0.5 \sum_{\mathrm{X}\in\mathcal{L}_{\mathrm{c}}} \sum_{\substack{\mathrm{Y}\neq\mathrm{X} \\ \mathrm{Y}\in\mathcal{L}_{\mathrm{c}}}} V_{\mathrm{XC}}^{\mathrm{X,Y}} - 0.5 \sum_{\mathrm{X}\in\mathcal{L}_{\mathrm{p}}} \sum_{\substack{\mathrm{Y}\neq\mathrm{X} \\ \mathrm{Y}\in\mathcal{L}_{\mathrm{p}}}} V_{\mathrm{XC}}^{\mathrm{X,Y}} \tag{S21}$$

Similar definitions would apply to the metal containing fragment

$$\Delta E_{\mathrm{int}}^{\mathcal{M}_{\mathrm{w}}} = \Delta V_{\mathrm{cl}}^{\mathcal{M}_{\mathrm{w}}} + \Delta V_{\mathrm{XC}}^{\mathcal{M}_{\mathrm{w}}} \tag{S22}$$

where

$$\Delta V_{\mathrm{cl}}^{\mathcal{M}_{\mathrm{w}}} = 0.5 \sum_{\mathrm{X}\in(\mathcal{M}_{\mathrm{w}})_{\mathrm{c}}} \sum_{\substack{\mathrm{Y}\neq\mathrm{X} \\ \mathrm{Y}\in(\mathcal{M}_{\mathrm{w}})_{\mathrm{c}}}} V_{\mathrm{cl}}^{\mathrm{X,Y}} - 0.5 \sum_{\mathrm{X}\in(\mathcal{M}_{\mathrm{w}})_{\mathrm{p}}} \sum_{\substack{\mathrm{Y}\neq\mathrm{X} \\ \mathrm{Y}\in(\mathcal{M}_{\mathrm{w}})_{\mathrm{p}}}} V_{\mathrm{cl}}^{\mathrm{X,Y}} \tag{S23}$$

and

$$\Delta V_{\mathrm{XC}}^{\mathcal{M}_{\mathrm{w}}} = 0.5 \sum_{\mathrm{X}\in(\mathcal{M}_{\mathrm{w}})_{\mathrm{c}}} \sum_{\substack{\mathrm{Y}\neq\mathrm{X} \\ \mathrm{Y}\in(\mathcal{M}_{\mathrm{w}})_{\mathrm{c}}}} V_{\mathrm{XC}}^{\mathrm{X,Y}} - 0.5 \sum_{\mathrm{X}\in(\mathcal{M}_{\mathrm{w}})_{\mathrm{p}}} \sum_{\substack{\mathrm{Y}\neq\mathrm{X} \\ \mathrm{Y}\in(\mathcal{M}_{\mathrm{w}})_{\mathrm{p}}}} V_{\mathrm{XC}}^{\mathrm{X,Y}} \tag{S24}$$

Equally important is an insight one can gain from classical and XC contributions making up the $E_{\mathrm{int}}^{(\mathcal{M}_{\mathrm{w}})_{\mathrm{c}},\mathcal{L}_{\mathrm{c}}}$ term and this can be easily computed from

$$E_{\mathrm{int}}^{(\mathcal{M}_{\mathrm{w}})_{\mathrm{c}},\mathcal{L}_{\mathrm{c}}} = V_{\mathrm{cl}}^{(\mathcal{M}_{\mathrm{w}})_{\mathrm{c}},\mathcal{L}_{\mathrm{c}}} + V_{\mathrm{XC}}^{(\mathcal{M}_{\mathrm{w}})_{\mathrm{c}},\mathcal{L}_{\mathrm{c}}} = \sum_{\mathrm{X}\in(\mathcal{M}_{\mathrm{w}})_{\mathrm{c}}} \sum_{\mathrm{Y}\in\mathcal{L}_{\mathrm{c}}} V_{\mathrm{cl}}^{\mathrm{X,Y}} + \sum_{\mathrm{X}\in(\mathcal{M}_{\mathrm{w}})_{\mathrm{c}}} \sum_{\mathrm{Y}\in\mathcal{L}_{\mathrm{c}}} V_{\mathrm{XC}}^{\mathrm{X,Y}} \tag{S25}$$

All the above is of great importance as it allows us to trace changes in primary IQA energy terms and their components which we hope will be of great help in tracking the origin and nature of factors controlling preferential affinity between two fragments, $\mathcal{M}_{\mathrm{w}}$ and $\mathcal{L}$, in both complexes, hence also should explain relative stability of molecular systems.

Finally, it is also of interest and importance to recover the terms defined in the IQF approach. To achieve that, let us first recall that in the IQA framework, the deformation energy of an atom is defined as the change in the self-energy of an atom X, $E_{\mathrm{def}}^{\mathrm{X}} = \Delta E_{\mathrm{self}}^{\mathrm{X}} = E_{\mathrm{self}}^{\mathrm{X}} - E_{\mathrm{vac}}^{\mathrm{X}}$, where the last term typically represents the energy of an atom *in vacuo*. Because there are two fragments in the molecular system investigate here, the polyatomic $\mathcal{L}$ and $\mathcal{M}_{\mathrm{w}}$, the energy contribution due to the change in self-atomic energies ($\Delta E_{\mathrm{self}}^{\mathrm{ML}}$) can be conveniently divided into those for each atom of the ligand, $\Delta E_{\mathrm{self}}^{\mathcal{L}}$, when it changes from the $\mathcal{L}_{\mathrm{p}}$ to $\mathcal{L}_{\mathrm{c}}$ state and those of each atom of the metal fragment $\Delta E_{\mathrm{self}}^{\mathcal{M}}$ when it changes to its $(\mathcal{M}_{\mathrm{w}})_{\mathrm{p}}$ to $(\mathcal{M}_{\mathrm{w}})_{\mathrm{c}}$ state.

$$\Delta E_{\text{self}}^{\text{ML}} = \Delta E_{\text{self}}^{\mathcal{M}_{\text{w}}} + \Delta E_{\text{self}}^{\mathcal{L}} \tag{S26}$$

where

$$\Delta E_{\text{self}}^{\mathcal{M}_{\text{w}}} = \sum_{\text{X}\in(\mathcal{M}_{\text{w}})_{\text{c}}} E_{\text{self}}^{\text{X}} - \sum_{\text{X}\in(\mathcal{M}_{\text{w}})_{\text{p}}} E_{\text{self}}^{\text{X}} = E_{\text{self}}^{(\mathcal{M}_{\text{w}})_{\text{c}}} - E_{\text{self}}^{(\mathcal{M}_{\text{w}})_{\text{p}}} \tag{S27}$$

and

$$\Delta E_{\text{self}}^{\mathcal{L}} = \sum_{\text{X}\in\mathcal{L}_{\text{c}}} E_{\text{self}}^{\text{X}} - \sum_{\text{X}\in\mathcal{L}_{\text{p}}} E_{\text{self}}^{\text{X}} = E_{\text{self}}^{\mathcal{L}_{\text{c}}} - E_{\text{self}}^{\mathcal{L}_{\text{p}}} \tag{S28}$$

According to the IQF framework, the deformation energy of a fragment is defined as the sum of the atomic deformation energies within a fragment and the sum of all unique interaction energies within the fragment when separated atoms form a molecule. Because in our case free atoms are not used as a reference state to monitor changes in $\mathcal{L}$, we express the deformation energy of $\mathcal{L}$ as a difference in the net energies of fragments $\mathcal{L}_{\text{c}}$ and $\mathcal{L}_{\text{p}}$,

$$E_{\text{def}}^{\mathcal{L}} = E_{\text{net}}^{\mathcal{L}_{\text{c}}} - E_{\text{net}}^{\mathcal{L}_{\text{p}}} = \left(E_{\text{self}}^{\mathcal{L}_{\text{c}}} + E_{\text{int}}^{\mathcal{L}_{\text{c}}}\right) - \left(E_{\text{self}}^{\mathcal{L}_{\text{p}}} + E_{\text{int}}^{\mathcal{L}_{\text{p}}}\right) = \Delta E_{\text{self}}^{\mathcal{L}} + \Delta E_{\text{int}}^{\mathcal{L}}. \tag{S29}$$

$$E_{\text{def}}^{\mathcal{M}_{\text{w}}} = E_{\text{net}}^{(\mathcal{M}_{\text{w}})_{\text{c}}} - E_{\text{net}}^{(\mathcal{M}_{\text{w}})_{\text{p}}} = \left(E_{\text{self}}^{(\mathcal{M}_{\text{w}})_{\text{c}}} + E_{\text{int}}^{(\mathcal{M}_{\text{w}})_{\text{c}}}\right) - \left(E_{\text{self}}^{(\mathcal{M}_{\text{w}})_{\text{p}}} + E_{\text{int}}^{(\mathcal{M}_{\text{w}})_{\text{p}}}\right) = \Delta E_{\text{self}}^{\mathcal{M}_{\text{w}}} + \Delta E_{\text{int}}^{\mathcal{M}_{\text{w}}}. \tag{S30}$$

Thus, the binding energy for a metal complex can be expressed within the IQF framework as the sum of the deformation energies of the individual fragments and the interaction energy between the two fragments (intra-fragment interaction energy term) and by substituting Eq. (S26), (S29) and (S30) into Eq. (S16) we obtain

$$E_{\text{bind}}^{\text{ML}} = \Delta E_{\text{self}}^{\mathcal{M}_{\text{w}}} + \Delta E_{\text{self}}^{\mathcal{L}} + \Delta E_{\text{int}}^{\mathcal{M}_{\text{w}}} + \Delta E_{\text{int}}^{\mathcal{L}} + E_{\text{int}}^{\mathcal{M}_{\text{c}},\mathcal{L}_{\text{c}}} = E_{\text{def}}^{\mathcal{M}_{\text{w}}} + E_{\text{def}}^{\mathcal{L}} + E_{\text{int}}^{\mathcal{M}_{\text{c}},\mathcal{L}_{\text{c}}} \tag{S31}$$

Comparing Eq. (S31) and (S16), the decomposition of the E_{bind} in Eq. (S31) refocuses the IQA-defined components into IQF related components; the contribution of intra-atomic energies, $\Delta E_{\text{self}}^{\text{ML}}$, and the contribution of diatomic interactions within a particular fragment, $\Delta E_{\text{int}}^{\mathcal{M}_{\text{w}}}$ and $\Delta E_{\text{int}}^{\mathcal{L}}$, are expressed in terms of relevant deformation energy terms, which, as will be seen from discussion that follows, makes the interpretation of relevant stability of molecular systems much easier and convincing.

End of PART S4

Table S9. Analysis of interaction energies (in kcal/mol) contributing to $E_{\mathrm{int}}^{\mathcal{M}_{\mathrm{C}}(\mathcal{W}_2)_{\mathrm{C}}}$ in both complexes.

ZnNTPA					ZnNTA				
Atom X	Atom Y	$V_{\mathrm{cl}}^{\mathrm{X,Y}}$	$V_{\mathrm{XC}}^{\mathrm{X,Y}}$	$E_{\mathrm{int}}^{\mathrm{X,Y}}$	Atom X	Atom Y	$V_{\mathrm{cl}}^{\mathrm{X,Y}}$	$V_{\mathrm{XC}}^{\mathrm{X,Y}}$	$E_{\mathrm{int}}^{\mathrm{X,Y}}$
O31($\mathcal{W}_2^a$)	O25(b)	161.4	–7.6	153.7	O22($\mathcal{W}_2^a$)	O19(b)	154.5	–6.1	148.4
O31($\mathcal{W}_2^a$)	O28(b)	158.9	–6.8	152.1	O22($\mathcal{W}_2^a$)	O15(b)	137.4	–2.1	135.3
O31($\mathcal{W}_2^a$)	O22(b)	140.9	–3.0	137.9	O22($\mathcal{W}_2^a$)	O13(b)	134.7	–2.1	132.6
O31($\mathcal{W}_2^a$)	O24(nb)	100.2	–0.1	100.1	O22($\mathcal{W}_2^a$)	O18(nb)	94.1	–0.1	94.0
O31($\mathcal{W}_2^a$)	O27(nb)	97.1	–0.1	97.0	O22($\mathcal{W}_2^a$)	N4	91.7	–0.1	91.7
O31($\mathcal{W}_2^a$)	O21(nb)	94.0	–0.1	93.9	H24($\mathcal{W}_2^a$)	γC17	88.1	0.0	88.0
H32($\mathcal{W}_2^a$)	γC23	93.7	0.0	93.6	O22($\mathcal{W}_2^a$)	O16(nb)	87.6	0.0	87.6
H33($\mathcal{W}_2^a$)	γC26	88.9	0.0	88.9	O22($\mathcal{W}_2^a$)	O12(nb)	86.4	0.0	86.4
O31($\mathcal{W}_2^a$)	N4	87.4	0.0	87.4	H24($\mathcal{W}_2^a$)	γC14	71.5	0.0	71.5
H32($\mathcal{W}_2^a$)	γC26	74.9	0.0	74.9	H23($\mathcal{W}_2^a$)	γC14	71.4	0.0	71.4
H33($\mathcal{W}_2^a$)	γC23	73.4	0.0	73.4	H23($\mathcal{W}_2^a$)	γC17	69.1	0.0	69.1
H33($\mathcal{W}_2^a$)	γC20	73.2	0.0	73.2	H24($\mathcal{W}_2^a$)	γC11	67.5	0.0	67.5
H32($\mathcal{W}_2^a$)	γC20	65.8	0.0	65.7	H23($\mathcal{W}_2^a$)	γC11	65.2	0.0	65.2
H32($\mathcal{W}_2^a$)	αC8	13.2	0.0	13.2	H24($\mathcal{W}_2^a$)	αC5	13.1	0.0	13.1
H32($\mathcal{W}_2^a$)	αC5	12.7	0.0	12.7	H24($\mathcal{W}_2^a$)	αC8	12.9	0.0	12.9
H33($\mathcal{W}_2^a$)	αC5	12.7	0.0	12.7	H24($\mathcal{W}_2^a$)	αC1	12.9	0.0	12.9
H32($\mathcal{W}_2^a$)	αC1	12.5	0.0	12.5	H23($\mathcal{W}_2^a$)	αC8	12.4	0.0	12.4
H33($\mathcal{W}_2^a$)	αC1	12.4	0.0	12.4	H23($\mathcal{W}_2^a$)	αC1	12.3	0.0	12.3
H33($\mathcal{W}_2^a$)	αC8	12.4	0.0	12.4	H23($\mathcal{W}_2^a$)	αC5	11.7	0.0	11.7
Sum(kcal/mol):		*1385.4*	*–17.9*	*1367.6*	*Sum(kcal/mol):*		*1294.5*	*–10.5*	*1284.0*
O31($\mathcal{W}_2^a$)	αC5	–24.6	0.0	–24.6	O22($\mathcal{W}_2^a$)	αC5	–24.8	0.0	–24.8
O31($\mathcal{W}_2^a$)	αC1	–24.7	0.0	–24.7	O22($\mathcal{W}_2^a$)	αC8	–25.1	0.0	–25.1
O31($\mathcal{W}_2^a$)	αC8	–25.0	0.0	–25.0	O22($\mathcal{W}_2^a$)	αC1	–25.4	0.0	–25.4
H32($\mathcal{W}_2^a$)	O21(nb)	–43.7	0.0	–43.7	H23($\mathcal{W}_2^a$)	O12(nb)	–42.2	0.0	–42.2
H33($\mathcal{W}_2^a$)	N4	–43.8	0.0	–43.8	H24($\mathcal{W}_2^a$)	O12(nb)	–43.3	0.0	–43.3
H32($\mathcal{W}_2^a$)	N4	–45.0	0.0	–45.0	H23($\mathcal{W}_2^a$)	N4	–44.1	0.0	–44.1
H32($\mathcal{W}_2^a$)	O27(nb)	–48.2	0.0	–48.2	H23($\mathcal{W}_2^a$)	O18(nb)	–44.3	0.0	–44.3
H33($\mathcal{W}_2^a$)	O24(nb)	–48.4	0.0	–48.4	H23($\mathcal{W}_2^a$)	O16(nb)	–45.7	0.0	–45.7
H33($\mathcal{W}_2^a$)	O21(nb)	–49.1	0.0	–49.1	H24($\mathcal{W}_2^a$)	O16(nb)	–45.9	0.0	–45.9
H33($\mathcal{W}_2^a$)	O27(nb)	–56.6	0.0	–56.6	H24($\mathcal{W}_2^a$)	N4	–47.1	0.0	–47.1
H32($\mathcal{W}_2^a$)	O24(nb)	–60.8	0.0	–60.9	H24($\mathcal{W}_2^a$)	O18(nb)	–54.9	0.0	–54.9
H32($\mathcal{W}_2^a$)	O22(b)	–63.6	0.0	–63.6	H23($\mathcal{W}_2^a$)	O13(b)	–62.3	0.0	–62.3
H33($\mathcal{W}_2^a$)	O22(b)	–69.9	0.0	–69.9	H24($\mathcal{W}_2^a$)	O13(b)	–65.3	0.0	–65.3
H33($\mathcal{W}_2^a$)	O25(b)	–74.7	–0.1	–74.7	H23($\mathcal{W}_2^a$)	O19(b)	–67.6	–0.1	–67.8
H32($\mathcal{W}_2^a$)	O28(b)	–74.9	–0.1	–75.0	H24($\mathcal{W}_2^a$)	O15(b)	–69.3	0.0	–69.3
H33($\mathcal{W}_2^a$)	O28(b)	–95.2	–1.9	–97.1	H23($\mathcal{W}_2^a$)	O15(b)	–70.9	0.0	–70.9
H32($\mathcal{W}_2^a$)	O25(b)	–101.0	–3.2	–104.1	H24($\mathcal{W}_2^a$)	O19(b)	–93.1	–1.1	–94.2
O31($\mathcal{W}_2^a$)	γC20	–142.5	–0.1	–142.6	O22($\mathcal{W}_2^a$)	γC11	–136.5	–0.1	–136.6
O31($\mathcal{W}_2^a$)	γC26	–152.5	–0.1	–152.6	O22($\mathcal{W}_2^a$)	γC14	–138.7	–0.1	–138.7
O31($\mathcal{W}_2^a$)	γC23	–154.2	–0.2	–154.3	O22($\mathcal{W}_2^a$)	γC17	–151.0	–0.1	–151.1
*Sum(*kcalmol^{-1}*):*		*–1398.2*	*–5.7*	*–1403.9*	*Sum(*kcalmol^{-1}*):*		*–1297.5*	*–1.6*	*–1299.1*
Total (kcalmol^{-1}):		**–11.9**	**–23.8**	**–35.7**	**Total (kcalmol^{-1}):**		**–2.9**	**–12.2**	**–15.1**

Table S10. IQA partitioning of two-bodied interaction energies of all interactions with the O-atom in ZnNTPA and ZnNTA using the XL3YP wavefunction on the MP2 structures.

ZnNTPA					ZnNTA				
Atoms		$V_{cl}^{X,Y}$	$V_{XC}^{X,Y}$	$E_{int}^{X,Y}$	Atoms		$V_{cl}^{X,Y}$	$V_{XC}^{X,Y}$	$E_{int}^{X,Y}$
X	Y				X	Y			
O30	C1	–32.9	–0.2	–33.1	O21	C1	–33.8	–0.7	-34.5
O30	H2	–2.1	0.0	–2.1	O21	H2	–4.1	0.0	-4.1
O30	H3	–1.9	–0.6	–2.5	O21	H3	–4.8	–1.1	-5.9
O30	N4	110.0	–0.7	109.3	O21	N4	114.4	–0.9	113.5
O30	C5	–27.3	0.0	–27.4	O21	C5	–27.0	0.0	-27.0
O30	H6	–2.0	0.0	–2.0	O21	H6	–3.3	0.0	-3.3
O30	H7	–2.2	0.0	–2.2	O21	H7	–3.8	0.0	-3.8
O30	C8	–35.0	–1.1	–36.0	O21	C8	–32.3	–0.2	-32.5
O30	H9	–2.3	–0.1	–2.4	O21	H9	–4.0	0.0	-4.0
O30	H10	–1.5	–3.3	–4.8	O21	H10	–4.6	–0.2	-4.8
O30	C11	–1.5	–0.1	–1.5	O21	C11	–171.5	–0.4	-171.8
O30	H12	–2.9	0.0	–3.0	O21	O12	108.4	–0.1	108.3
O30	C13	–1.4	0.0	–1.5	O21	O13	152.9	–5.6	147.3
O30	H14	–2.0	0.0	–2.0	O21	C14	–165.2	–0.2	-165.4
O30	C15	–1.6	0.0	–1.6	O21	O15	156.1	–6.7	149.5
O30	H16	–2.9	0.0	–3.0	O21	O16	102.1	–0.1	102.0
O30	H17	–2.7	0.0	–2.7	O21	C17	–117.7	0.0	-117.7
O30	H18	–1.8	0.0	–1.8	O21	O18	75.7	0.0	75.7
O30	H19	–3.5	0.0	–3.5	O21	O19	104.0	0.0	104.0
O30	C20	–159.4	–0.2	–159.6	Sum (kcalmol^{-1}):		241.8	–16.3	225.5
O30	O21	100.2	–0.1	100.1					
O30	O22	163.4	–9.2	154.2					
O30	C23	–164.5	–0.2	–164.7					
O30	O24	105.8	–0.1	105.7					
O30	O25	154.7	–5.9	148.8					
O30	C26	–110.1	0.0	–110.1					
O30	O27	72.8	0.0	72.8					
O30	O28	102.6	0.0	102.6					
Sum (kcalmol^{-1}):		247.8	–21.8	226.0					

Table S11. IQA partitioning of two-bodied interaction energies of all interactions with the O-atom in ZnNTPA and ZnNTA using the XL3YP wavefunction on the MP2 structures.

ZnNTPA					ZnNTA				
Atoms		$V_{cl}^{X,Y}$	$V_{XC}^{X,Y}$	$E_{int}^{X,Y}$	Atoms		$V_{cl}^{X,Y}$	$V_{XC}^{X,Y}$	$E_{int}^{X,Y}$
X	Y				X	Y			
O31	C1	–24.7	0.0	–24.7	O22	C1	–25.4	0.0	–25.4
O31	H2	–1.4	0.0	–1.4	O22	H2	–2.8	0.0	–2.8
O31	H3	–2.0	0.0	–2.0	O22	H3	–3.7	0.0	–3.7
O31	N4	87.4	0.0	87.4	O22	N4	91.7	–0.1	91.7
O31	C5	–24.6	0.0	–24.6	O22	C5	–24.8	0.0	–24.8
O31	H6	–2.0	0.0	–2.0	O22	H6	–3.3	0.0	–3.3
O31	H7	–2.0	0.0	–2.0	O22	H7	–3.7	0.0	–3.7
O31	C8	–25.0	0.0	–25.0	O22	C8	–25.1	0.0	–25.1
O31	H9	–1.4	0.0	–1.4	O22	H9	–3.0	0.0	–3.0
O31	H10	–1.8	0.0	–1.8	O22	H10	–3.7	0.0	–3.7
O31	C11	–1.2	0.0	–1.3	O22	C11	–136.5	–0.1	–136.6
O31	H12	–2.1	0.0	–2.1	O22	O12	86.4	0.0	86.4
O31	C13	–1.5	0.0	–1.5	O22	O13	134.7	–2.1	132.6
O31	H14	–2.4	0.0	–2.4	O22	C14	–138.7	–0.1	–138.7
O31	C15	–1.1	0.0	–1.2	O22	O15	137.4	–2.1	135.3
O31	H16	–2.5	0.0	–2.5	O22	O16	87.6	0.0	87.6
O31	H17	–2.0	0.0	–2.0	O22	C17	–151.0	–0.1	–151.1
O31	H18	–2.0	0.0	–2.0	O22	O18	94.1	–0.1	94.0
O31	H19	–2.8	0.0	–2.8	O22	O19	154.5	–6.1	148.4
O31	C20	–142.5	–0.1	–142.6	Sum (kcalmol^{-1}):		265.0	–10.8	254.2
O31	O21	94.0	–0.1	93.9					
O31	O22	140.9	–3.0	137.9					
O31	C23	–154.2	–0.2	–154.3					
O31	O24	100.2	–0.1	100.1					
O31	O25	161.4	–7.6	153.7					
O31	C26	–152.5	–0.1	–152.6					
O31	O27	97.1	–0.1	97.0					
O31	O28	158.9	–6.8	152.1					
Sum (kcalmol^{-1}):		288.1	–18.3	269.9					

Table S12. IQA partitioning of two-bodied interaction energies of all interactions with the H-atom in ZnNTPA and ZnNTA using the XL3YP wavefunction on the MP2 structures.

ZnNTPA					ZnNTA				
Atoms		$V_{cl}^{X,Y}$	$V_{XC}^{X,Y}$	$E_{int}^{X,Y}$	Atoms		$V_{cl}^{X,Y}$	$V_{XC}^{X,Y}$	$E_{int}^{X,Y}$
X	Y				X	Y			
H32	C1	12.5	0.0	12.5	H23	C1	12.3	0.0	12.3
H32	H2	0.7	0.0	0.7	H23	H2	1.4	0.0	1.4
H32	H3	1.0	0.0	1.0	H23	H3	1.8	0.0	1.8
H32	N4	–45.0	0.0	–45.0	H23	N4	–44.1	0.0	-44.1
H32	C5	12.7	0.0	12.7	H23	C5	11.7	0.0	11.7
H32	H6	1.0	0.0	1.0	H23	H6	1.5	0.0	1.5
H32	H7	1.1	0.0	1.1	H23	H7	1.8	0.0	1.8
H32	C8	13.2	0.0	13.2	H23	C8	12.4	0.0	12.4
H32	H9	0.8	0.0	0.8	H23	H9	1.5	0.0	1.5
H32	H10	0.9	0.0	0.9	H23	H10	1.8	0.0	1.8
H32	C11	0.7	0.0	0.6	H23	C11	65.2	0.0	65.2
H32	H12	1.2	0.0	1.2	H23	O12	–42.2	0.0	-42.2
H32	C13	0.8	0.0	0.8	H23	O13	–62.3	0.0	-62.3
H32	H14	1.2	0.0	1.2	H23	C14	71.4	0.0	71.4
H32	C15	0.6	0.0	0.6	H23	O15	–70.9	0.0	-70.9
H32	H16	1.2	0.0	1.2	H23	O16	–45.7	0.0	-45.7
H32	H17	1.0	0.0	1.0	H23	C17	69.1	0.0	69.1
H32	H18	1.0	0.0	1.0	H23	O18	–44.3	0.0	-44.3
H32	H19	1.6	0.0	1.6	H23	O19	–67.6	–0.1	-67.8
H32	C20	65.8	0.0	65.7	Sum (kcalmol^{-1}):		–125.3	–0.2	–125.5
H32	O21	–43.7	0.0	–43.7					
H32	O22	–63.6	0.0	–63.6					
H32	C23	93.7	0.0	93.6					
H32	O24	–60.8	0.0	–60.9					
H32	O25	–101.0	–3.2	–104.1					
H32	C26	74.9	0.0	74.9					
H32	O27	–48.2	0.0	–48.2					
H32	O28	–74.9	–0.1	–75.0					
Sum (kcalmol^{-1}):		–149.8	–3.4	–153.2					

Table S13. IQA partitioning of two-bodied interaction energies of all interactions with the H-atom in ZnNTPA and ZnNTA using the XL3YP wavefunction on the MP2 structures.

ZnNTPA					ZnNTA				
Atoms		$V_{cl}^{X,Y}$	$V_{XC}^{X,Y}$	$E_{int}^{X,Y}$	Atoms		$V_{cl}^{X,Y}$	$V_{XC}^{X,Y}$	$E_{int}^{X,Y}$
X	Y				X	Y			
H33	C1	12.4	0.0	12.4	H24	C1	12.9	0.0	12.9
H33	H2	0.7	0.0	0.7	H24	H2	1.4	0.0	1.4
H33	H3	1.0	0.0	1.0	H24	H3	1.8	0.0	1.8
H33	N4	–43.8	0.0	–43.8	H24	N4	–47.1	0.0	–47.1
H33	C5	12.7	0.0	12.7	H24	C5	13.1	0.0	13.1
H33	H6	1.0	0.0	1.0	H24	H6	1.8	0.0	1.8
H33	H7	1.0	0.0	1.0	H24	H7	2.0	0.0	2.0
H33	C8	12.4	0.0	12.4	H24	C8	12.9	0.0	12.9
H33	H9	0.7	0.0	0.7	H24	H9	1.5	0.0	1.5
H33	H10	0.9	0.0	0.9	H24	H10	1.9	0.0	1.9
H33	C11	0.6	0.0	0.6	H24	C11	67.5	0.0	67.5
H33	H12	1.0	0.0	1.0	H24	O12	–43.3	0.0	–43.3
H33	C13	0.9	0.0	0.9	H24	O13	–65.3	0.0	–65.3
H33	H14	1.3	0.0	1.3	H24	C14	71.5	0.0	71.5
H33	C15	0.5	0.0	0.5	H24	O15	–69.3	0.0	–69.3
H33	H16	1.3	0.0	1.3	H24	O16	–45.9	0.0	–45.9
H33	H17	1.0	0.0	1.0	H24	C17	88.1	0.0	88.0
H33	H18	1.1	0.0	1.1	H24	O18	–54.9	0.0	–54.9
H33	H19	1.4	0.0	1.4	H24	O19	–93.1	–1.1	–94.2
H33	C20	73.2	0.0	73.2	Sum (kcalmol^{-1}):		–142.5	–1.2	–143.7
H33	O21	–49.1	0.0	–49.1					
H33	O22	–69.9	0.0	–69.9					
H33	C23	73.4	0.0	73.4					
H33	O24	–48.4	0.0	–48.4					
H33	O25	–74.7	–0.1	–74.7					
H33	C26	88.9	0.0	88.9					
H33	O27	–56.6	0.0	–56.6					
H33	O28	–95.2	–1.9	–97.1					
Sum (kcalmol^{-1}):		–150.3	–2.1	–152.4					

Table S14. IQA partitioning of two-bodied interaction energies of all interactions with the H-atom in ZnNTPA and ZnNTA using the XL3YP wavefunction on the MP2 structures.

ZnNTPA					ZnNTA				
Atoms		$V_{cl}^{X,Y}$	$V_{XC}^{X,Y}$	$E_{int}^{X,Y}$	Atoms		$V_{cl}^{X,Y}$	$V_{XC}^{X,Y}$	$E_{int}^{X,Y}$
X	Y				X	Y			
H34	C1	17.1	0.0	17.1	H25	C1	15.9	0.0	15.9
H34	H2	1.2	0.0	1.2	H25	H2	1.9	0.0	1.9
H34	H3	0.9	–0.1	0.8	H25	H3	2.3	0.0	2.3
H34	N4	–54.5	0.0	–54.5	H25	N4	–52.3	0.0	-52.3
H34	C5	13.6	0.0	13.6	H25	C5	12.7	0.0	12.7
H34	H6	1.0	0.0	1.0	H25	H6	1.5	0.0	1.5
H34	H7	1.1	0.0	1.1	H25	H7	1.8	0.0	1.8
H34	C8	16.9	0.0	16.9	H25	C8	14.5	0.0	14.5
H34	H9	1.0	0.0	1.0	H25	H9	1.8	0.0	1.8
H34	H10	0.7	0.0	0.7	H25	H10	2.1	0.0	2.0
H34	C11	0.8	0.0	0.8	H25	C11	91.0	0.0	90.9
H34	H12	1.3	0.0	1.3	H25	O12	–58.5	0.0	-58.5
H34	C13	0.7	0.0	0.7	H25	O13	–82.1	–0.2	-82.3
H34	H14	1.0	0.0	1.0	H25	C14	72.0	0.0	72.0
H34	C15	0.9	0.0	0.9	H25	O15	–66.2	–0.2	-66.3
H34	H16	1.6	0.0	1.6	H25	O16	–46.1	0.0	-46.1
H34	H17	1.5	0.0	1.5	H25	C17	57.1	0.0	57.1
H34	H18	0.9	0.0	0.9	H25	O18	–37.1	0.0	-37.1
H34	H19	1.6	0.0	1.6	H25	O19	–50.4	0.0	-50.4
H34	C20	94.8	0.0	94.7	Sum (kcalmol^{-1}):		–118.2	–0.4	–118.6
H34	O21	–59.0	0.0	–59.0					
H34	O22	–98.9	–2.0	–100.8					
H34	C23	71.9	0.0	71.9					
H34	O24	–47.3	0.0	–47.3					
H34	O25	–66.1	–0.1	–66.3					
H34	C26	55.4	0.0	55.4					
H34	O27	–36.9	0.0	–36.9					
H34	O28	–51.6	0.0	–51.6					
Sum (kcalmol^{-1}):		–128.3	–2.3	–130.6					

Table S15. IQA partitioning of two-bodied interaction energies of all interactions with the H-atom in ZnNTPA and ZnNTA using the XL3YP wavefunction on the MP2 structures.

ZnNTPA					ZnNTA				
Atoms		$V_{cl}^{X,Y}$	$V_{XC}^{X,Y}$	$E_{int}^{X,Y}$	Atoms		$V_{cl}^{X,Y}$	$V_{XC}^{X,Y}$	$E_{int}^{X,Y}$
X	Y				X	Y			
H35	C1	15.5	0.0	15.5	H26	C1	15.7	0.0	15.7
H35	H2	0.9	0.0	0.9	H26	H2	1.8	0.0	1.8
H35	H3	0.9	0.0	0.9	H26	H3	2.2	0.0	2.2
H35	N4	–51.9	0.0	–51.9	H26	N4	–54.3	0.0	-54.3
H35	C5	13.2	0.0	13.2	H26	C5	13.0	0.0	13.0
H35	H6	0.9	0.0	0.9	H26	H6	1.6	0.0	1.6
H35	H7	1.1	0.0	1.1	H26	H7	1.8	0.0	1.8
H35	C8	17.4	–0.1	17.3	H26	C8	16.0	0.0	16.0
H35	H9	1.2	0.0	1.2	H26	H9	2.1	0.0	2.1
H35	H10	0.7	–0.2	0.5	H26	H10	2.3	0.0	2.3
H35	C11	0.7	0.0	0.7	H26	C11	74.8	0.0	74.8
H35	H12	1.6	0.0	1.6	H26	O12	–48.7	0.0	-48.7
H35	C13	0.7	0.0	0.7	H26	O13	–65.2	-0.1	-65.3
H35	H14	1.0	0.0	1.0	H26	C14	92.4	0.0	92.4
H35	C15	0.7	0.0	0.7	H26	O15	–89.1	-0.6	-89.7
H35	H16	1.3	0.0	1.3	H26	O16	–57.4	0.0	-57.4
H35	H17	1.2	0.0	1.2	H26	C17	58.7	0.0	58.7
H35	H18	0.9	0.0	0.9	H26	O18	–38.2	0.0	-38.2
H35	H19	1.8	0.0	1.8	H26	O19	–51.7	0.0	-51.7
H35	C20	69.4	0.0	69.4	Sum (kcalmol^{-1}):		–122.3	–0.8	-123.1
H35	O21	–45.0	0.0	–45.1					
H35	O22	–67.6	–0.2	–67.8					
H35	C23	87.6	0.0	87.6					
H35	O24	–57.7	0.0	–57.7					
H35	O25	–78.5	–0.1	–78.6					
H35	C26	51.7	0.0	51.7					
H35	O27	–34.6	0.0	–34.6					
H35	O28	–47.1	0.0	–47.1					
Sum (kcalmol^{-1}):		–112.0	–0.6	–112.7					